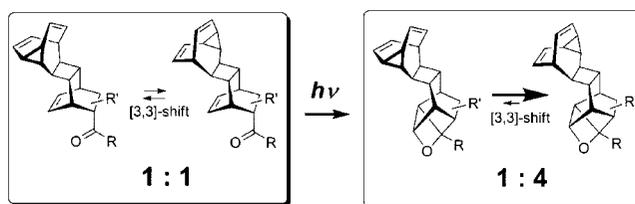# Effect of Intramolecular Paternò−Büchi Reaction on the Thermodynamics and Kinetics of Nearly Degenerate [3,3]-Sigmatropic Shift in Fluxional Polycycles

Roman A. Valiulin, Donald G. Dressen, Jennifer R. Riggs, Faven M. Habte, and Andrei G. Kutateladze*

Department of Chemistry and Biochemistry, University of Denver, Denver, Colorado 80208

akutatel@du.edu

In reactions with weak dienophiles, cyclooctatetraene (COT) often yields 2:1 adducts possessing the fluxional bicyclo[5.1.0]octadiene moiety. They undergo fast, nearly degenerate Cope rearrangement with an activation barrier similar to that of the parent dihydrobullvalene. Irradiation to excite the carbonyl moiety induces an intramolecular Paternò−Büchi cyclization yielding *endo*-oxetanes and significantly changing the Cope-averaged NMR spectra. In this paper we examine the effect of skeletal distortion caused by intramolecular [2 + 2]-photoaddition on thermodynamics and the activation barrier of the [3,3]-sigmatropic tautomerism. Our finding is that such a distortion lifts the energetic degeneracy of the two valence tautomers, while not affecting the activation barrier.

Introduction

Cyclooctatetraene (COT, **1**) produces several known dimerization products, of which pentacyclo[9.3.2.0²,⁹.0³,⁸.0¹⁰,¹²]hexadeca-4,6,13,15-tetraene (**2**) is the major. It was first identified by Schröder[1] and later was confirmed to be a reactive diene in Diels−Alder cycloadditions.[2] It is also well-known that COT undergoes fast electrocyclic ring closure into its bicyclic valence tautomer **3**, but this electrocyclization is not thermodynamically favorable ($\Delta G° \approx 7$ kcal/mol[3,4]) and **3** is present at less than 0.01% at equilibrium. For the classic Diels−Alder reactions of COT, the ramification is that unless the dienophile is very reactive, a prominent example being the maleic anhydride addition yielding the tricyclo[4.2.2.0²,⁵]decane framework, cyclooctatetraene does not produce the 1:1 adducts. Reactions with weaker dienophiles require extended heating, which causes COT

to dimerize, subsequently yielding the Diels−Alder adducts of **2**. In our studies of intramolecular Paternò−Büchi reactions in polycyclic systems, we noted that simple unsaturated ketones, such as vinyl methyl ketone, are not reactive enough to form 1:1 adducts with cyclooctatetraene. In fact, endo-9-acetyltricyclo[4.2.2.0²,⁵]deca-3,7-diene, for which an intramolecular Paternò−Büchi reaction was first reported by Sauers,[5] was obtained not via the reaction of vinyl methyl ketone with COT but rather via a two-step procedure: first, a low-yielding reaction of acrylonitrile with COT, followed by a methyl magnesium bromide reaction with the tricyclic nitrile.

COT dimer **2** is also known to undergo further intramolecular cycloaddition (NMR analysis of this secondary product was first attempted by Moore[6]) or secondary dimerization,[2b] which renders it inactive as the diene component of the Diels−Alder reaction. Dimer **2** undergoes fast degenerate Cope rearrangement, which is not perturbed by the [4 + 2]-cycloaddition of nearly symmetric citraconic anhydride.[2a]

In this study we have examined the fluxional nature of the dihydrobullvalene fragment in the Diels−Alder adducts of **2**

(1) (a) Schroeder, G. *Chem. Ber.* **1964**, *97* (11), 3131−3139. (b) Schroeder, G. *Chem. Ber.* **1964**, *97* (11), 3140−3149.
(2) (a) Deshpande, R. R.; Gilbert, A.; Fray, G. I.; Saxton, R. G. *Tetrahedron Lett.* **1971**, *24*, 2163−6. (b) Fray, G. I.; Saxton, R. G. *Tetrahedron* **1978**, *34*, 2663−7. (c) Mori, A.; Kato, N.; Takeshita, H.; Kurahashi, Y.; Ito, M. *J. Chem. Soc., Chem. Commun.* **1994**, *7*, 869−70.
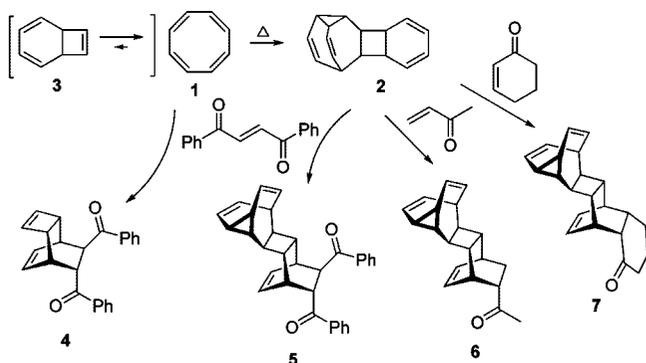(3) Huisgen, R.; Mietzsch, C. F. *Angew. Chem., Int. Ed. Engl.* **1964**, *3*, 83−84.
(4) Squillacote, M. E.; Bergman, A. *J. Org. Chem.* **1981**, *51*, 3911−3913.

(5) Sauers, R. R.; Rousseau, A. D.; Byrne, B. *J. Am. Chem. Soc.* **1975**, *97*, 4947−4953.
(6) Moore, H. W. *J. Am. Chem. Soc.* **1964**, *86* (16), 3398−3399.

SCHEME 1

SCHEME 2

5a, R = Ph, R' = exo-Bz   5b
6a, R = Me, R' = H   6b
7a, R,R' = -(CH₂)₃-endo   7b

$h\nu$

8a, R = Ph, R' = exo-Bz   8b
9a, R = Me, R' = H   9b
10a, R,R' = -(CH₂)₃-endo   10b

with unsaturated ketones and the effect of the intramolecular Paternò−Büchi [2 + 2]-cycloaddition on the thermodynamics and kinetics of the Cope valence tautomerism. As photoinduced oxetane formation distorts the mainly C_S-symmetric core, i.e., bicyclo[2.2.2]-structure, of Diels−Alder adducts, the rationale for these studies is to evaluate how such distortion affects the equilibrium and the activation barrier of the [3,3]-sigmatropic tautomerism. As we show here, it takes a very small structural distortion at the "business" dihydrobullvalene end of the molecule to dramatically change the NMR spectrum of this fluxional moiety due to the tilting of the potential energy surface, yet the rate of the two-state interconversion remains largely unaffected and fast. At the fundamental level, these are the desirable features of a switch where a photoinduced subtle perturbation causes a rapid amplified response from the system.

Results and Discussion

Vinyl methyl ketone is not a sufficiently reactive dienophile to form a 1:1 adduct with COT, even when taken in excess. Its solution with excess COT in dichlorobenzene was heated for 2 days at 180 °C, yielding 41% of the 2:1 adduct **6**. Cyclohexenone reacts similarly to furnish **7**, Scheme 1. *trans*-Dibenzoyl ethylene, a much better dienophile, can be reacted with COT in various ratios producing either 1:1 adduct **4** or 2:1 adduct **5**. (Ortep drawing of **5** is shown in Figure S5 in Supporting Information).

Although compounds **5**, **6**, and **7** possess similar features in NMR, we wanted to ensure that the structures **6** and **7** were also determined unambiguously. They were exhaustively characterized by NMR (¹H, ¹³C, COSY and NOE-differences) and additionally, the proton and ¹³C NMR spectra of **6** were modeled with density functional theory (DFT) using the B3LYP/6-311+G(d,p) optimized geometry and the mPW1PW91[7] GIAO-calculated chemical shifts and spin−spin coupling constants. For the single point calculations of the NMR properties, we have used increasingly complex basis sets 6-31G(d), 6-311+G(d,p), 6-311+G(2d,2p), and EPR-III.[8] We found that the best cost/performance compromise was achieved with the 6-311+G(d,p) basis set. Although EPR-III offered minor improvements, the CPU times were prohibitively long. There was very little difference in the quality of prediction with the 6-311+G(d,p) and 6-311+G(2d,2p) bases.

The 2:1 Diels−Alder adducts **5**, **6**, and **7** have two nearly isoenergetic Cope states. Their experimental spectra have
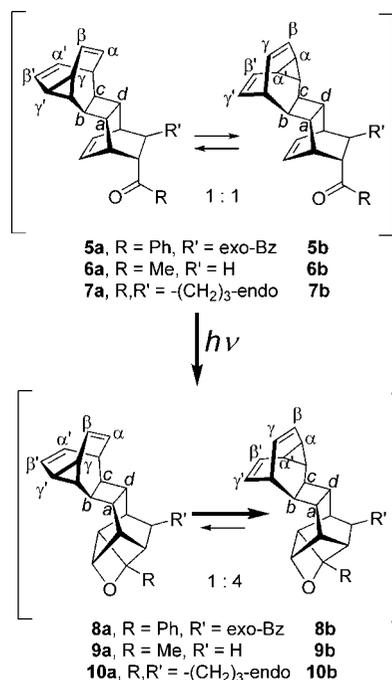
prominent broad peaks at 3.6−3.9 ppm, two cyclopropyl protons and two vinyl protons averaged by the Cope rearrangement ($\alpha \leftrightarrow \gamma$, $\alpha' \leftrightarrow \gamma'$). The calculated chemical shifts for each proton in the $\alpha-\gamma$ pairs of **6** support the observed averaging: the cyclopropane protons are calculated at 1.98 and 2.01 ppm, whereas the vinyl termini are calculated at 5.25 and 5.32 ppm. It is easy to see that the average of these calculated values (∼3.6 ppm) compares favorably with the experimental broad peak at 3.6−3.9 ppm. The other two protons of the divinyl-cyclopropyl moiety, β and β', which do not trade places during the rearrangement, appear as sharp triplets at 5.68 and 5.93 ppm. Similar 2:1 adducts of COT with other dienophiles **S-a**, **S-b**, **S-c**, and **S-d**[9] display the same prominent full averaging of protons α and γ in their NMR spectra (Supporting Information, pp S18−S23).

Irradiation of **5**−**7** with a broadband UV source, $\lambda = 300 \pm 50$ nm, produces oxetanes **8**, **9**, and **10**, Scheme 2, as evidenced by the disappearance of two low field multiplets of olefinic protons. As it was the case with the starting material, we were able to obtain the X-ray structure for the phenyl oxetane **8** (its Ortep drawing is shown in Figure S6 in Supporting Information).

Methyl oxetane **8** was characterized by ¹H, ¹³C, COSY. and NOE-diff, and its NMR was also simulated with the mPW1PW91/6-311+G(d,p)//B3LYP/6-311+G(d,p) density functional calculations. Figure 1 shows excellent correlation between the experimental and calculated chemical shifts.

In the experimental ¹H NMR spectrum of **9** (and **10**) the vinyl protons in the Cope moiety are not fully averaged with the cyclopropane protons, in contrast to complete averaging in the precursors **6** and **7** (Figure 2).

We hypothesize that the distortion of the polycyclic framework caused by the intramolecular Paternò−Büchi cyclization lifts the near degeneracy of the two Cope states. The oxetane formation occurs at the opposite end of the molecule and primarily affects its bicyclo[2.2.2]octane core. However, a minor

(7) Adamo, C.; Barone, V. *J. Chem. Phys.* **1998**, *108*, 664.
(8) Barone, V. In *Recent Advances in Density Functional Methods*, Part I; Chong, D. P., Ed.; World Scientific Publishing Co.: Singapore, 1996.

(9) The 2:1 adduct of COT with maleic anhydride **S-d** is previously described; see ref 1a.
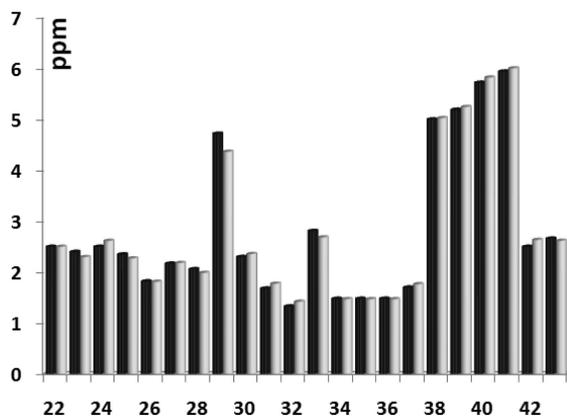
FIGURE 1. Correlation of experimental (dark bars) and calculated (light bars) proton chemical shifts in **9** (for numbering of protons 22−43 see Figure S7 in Supporting Information).

FIGURE 3. VT NMR experiment to determine the thermodynamic parameters of the **9a**−**9b** equilibrium.

distortion is propagated through the cyclobutane bridge, twisting the dihedral angle *a*−*b*−*c*−*d* (Scheme 2), which is calculated to be almost planar in the Diels−Alder adduct **6** (1.4°) but reaches 9.7° in the oxetane **9**. The X-ray structure of oxetane **8** shows very similar distortion, with the corresponding dihedral angle of 9.8°.

A less likely explanation for the lack of full Cope averaging in the oxetanes is that in the more rigid new framework the Cope rearrangement is slowed down to an intermediate exchange regime for the protons α−γ and α′−γ′, i.e., their corresponding peaks in the NMR spectrum move toward each other but are not fully coalesced. This is not in keeping with our experimental observations. Elevating the temperature from 20 to 160 °C in a VT NMR experiment showed that although the affected peaks migrated somewhat toward each other, even at the highest temperature there was no coalescence (see Figure S1 in Supporting Information).

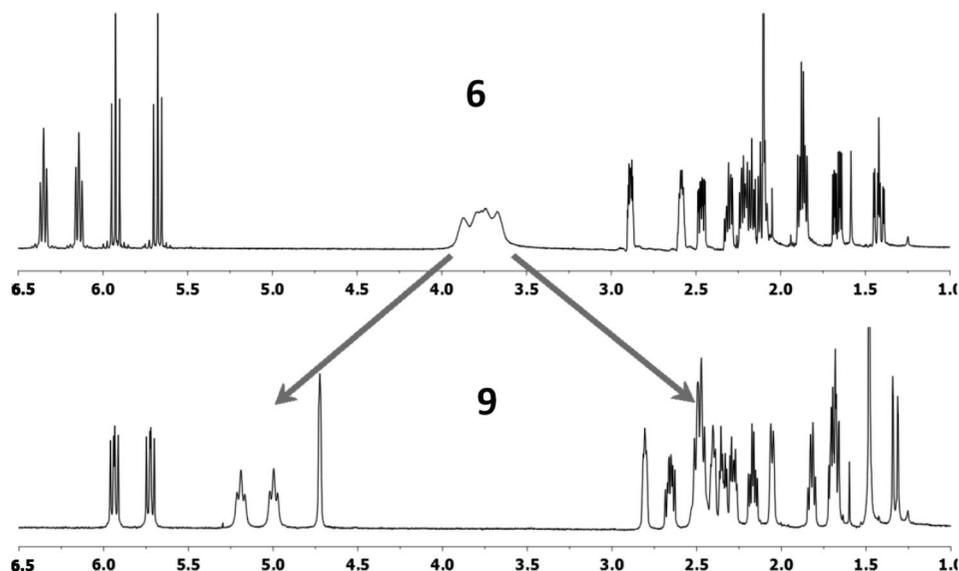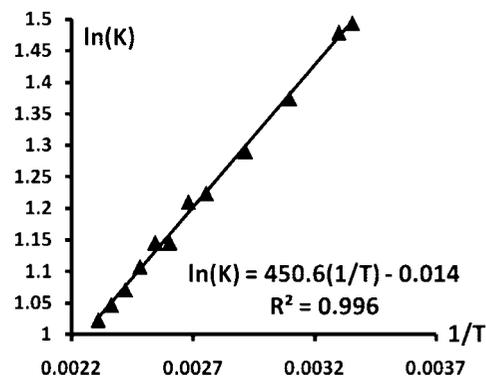Knowing that at 20 °C and above the respective protons are fully averaged, we used this VT experiment to determine the thermodynamic parameters for the equilibrium. The limiting values for the chemical shifts of protons α and γ, σ_o = 5.9 ppm for alkenyl and σ_∞ = 1.6 ppm for cyclopropyl, were obtained from the −100 °C low temperature NMR experiment described below.

The equilibrium constants at each temperature were calculated from the experimental chemical shifts (σ_{obs}) as $K = (\sigma_\infty - \sigma_{obs})/(\sigma_{obs} - \sigma_o)$ and plotted as the ln K against $1/T$, Figure 3. The activation enthalpy was obtained from the slope of this plot: ΔH = −slope·R = −0.89 ± 0.02 kcal/mol, and the activation entropy was obtained from the intercept ΔS = intercept·R = −0.03 ± 0.04 cal mol⁻¹ deg⁻¹. The enthalpy is in reasonably good agreement with the DFT-calculated energy difference of 0.51 kcal/mol (Table 1).

The experimental spectrum at 20 °C was simulated using the DFT chemical shifts weighted to account for the presence of both valence tautomers. When the weights for the two Cope forms **9a** and **9b** were calculated based on the equilibrium constant derived from the ZPE-corrected B3LYP/6-311+G(2d,2p) energy difference between the two isomers (ΔE = 0.51 kcal/mol, 29% and 71%), the resulting spectrum was very similar to the experimental. However, the simulation was further improved by mixing the two calculated spectra in a 1:4 ratio, which is in excellent agreement with the experimental ΔH and ΔS (which give 18%:82% at 25 °C).

Figure 4 illustrates the effect of different ratios of the Cope isomers **9a** and **9b** on the resulting average spectrum. As the fraction of the minor isomer **9a** increases, the two vinyl protons (green spots) move upfield, whereas the cyclopropyl protons (red spots) move downfield, improving the fit. The best fit (third panel) to the entire experimental spectrum corresponds to a ratio

FIGURE 2. NMR changes upon photoconversion of **6** to oxetane **8**.

TABLE 1. DFT Energies for the Diels−Alder Adducts 6, Paternò−Büchi Products 9, and Their Respective Cope Transition States

	[4 + 2] adduct **6**			Paternò−Büchi product **9**		
	6a	**6b**	**6ts**	**9a**	**9b**	**9ts**
B3LYP/6-31G(d)	−850.47770 (0.00)[a]	−850.47755 (0.09)	−850.46247 (9.6)	−850.44580 (0.56)	−850.44669 (0.00)	−850.43123 (9.7)
B3LYP/6-311+G(2d,2p)	−850.72454 (0.00)	−850.72455 (0.00)	−850.71084 (8.6)	−850.68525 (0.53)	−850.68609 (0.00)	−850.67259 (8.5)
B3LYP/6-311+G(2d,2p) ZPE-corrected	−850.35408 (0.01)	−850.35410 (0.00)	−850.34194 (7.6)	−850.31199 (0.51)	−850.31280 (0.00)	−850.30082 (7.5)

[a] Relative energies in kcal/mol for the triads **6a-6b-6ts** or **9a-9b-9ts** at a given theory level.
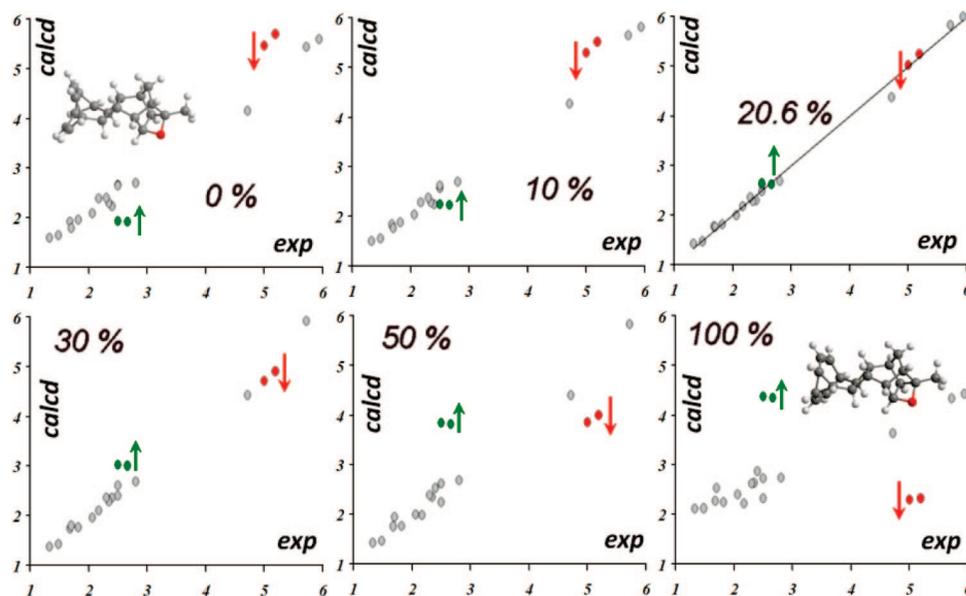

FIGURE 4. Correlation between the experimental and calculated proton chemical shifts for **9** as a function of the ratio of valence isomers **9a** and **9b**.

of 20.6:79.4, or $\Delta G = -0.78$ kcal/mol. Further "dilution" with **9a** deteriorates the fit, with both the green and the red pairs deviating from the best correlated values (panels 4−6, Figure 4).

The experimental ^{13}C NMR spectrum can also be simulated by "titrating" the calculated spectrum of **9b** with an increasing fraction of the second Cope tautomer **9a**. Prediction of the ^{13}C NMR spectrum also gives the approximate location of the Cope-averaged carbons, which are otherwise difficult to discern. For example, Figure 5 shows the predicted (top) and the experimental (bottom) ^{13}C NMR spectra of **9** based on the two calculated forms **9a** and **9b** weighted at 20.6:79.4. The four averaged carbon atoms (α,α' and γ,γ') in the calculated spectrum are identified by the asterisks, and their positions match small broad signals in the experimental spectrum (circled).

It appears that both experimental and computational evidence points to selective destabilization of one of the Cope states (**9a**) by the Paternò−Büchi photocyclization.

The question remains whether the rate of the valence interconversion is at all affected by this photoinduced structure distortion. To evaluate the effect of the intramolecular [2 + 2] cycloaddition on the activation barrier of the Cope rearrangement, we carried out low-temperature NMR studies of **6** and **9**, augmented by DFT calculations.

Because of the complexity of the spectrum, it is impossible to carry out the full dynamic NMR analysis to extract the rate constants and activation parameters. The α and γ protons averaged in the [3,3]-sigmatropic shift are separated by more than 4 ppm (1600 Hz), which makes the respective peaks at the coalescence temperature too broad for full modeling.

However, we were able to measure the coalescence temperature by analyzing other peaks in the spectra (Figures S1−S3 in Supporting Information). For the adduct **6** the coalescence temperature was approximately −72 to −74 °C, whereas for the Paternò−Büchi product **8** the coalescence temperature was slightly higher, approximately −65 °C, although the $\Delta\delta$ for the examined protons was higher in the case of **9**. Since the reaction rate at coalescence is related to the difference in the chemical shifts as $k = \pi\Delta\delta/\sqrt{2}$, we conclude that the free energies of activation are very similar for **6** and **9**. A very rough estimate using a modified Eyring equation, $\Delta G^{\ddagger} \approx 0.0046 T_C[10.2 + \ln(T_C/k)]$ kcal/mol,[10] gives approximately 8.5−10.5 kcal/mol, which is in good agreement with the reported values for dihydrobullvalene.[11,12]

Table 1 summarizes the results of the theoretical study. The last row in the table represents the most accurate level of theory where the energies are corrected for zero point vibrational energy. Both transition states **6ts** and **9ts** produced one imaginary frequency for which the normal mode corresponds to the reaction coordinate (i.e., the [3,3]-sigmatropic rearrangement). The main conclusion of this computational investigation is that the activation barriers for the Cope rearrangement in the Diels−Alder adduct **6** and the Paternò−Büchi product **9** are very similar, within 0.1 kcal/mol, and therefore the distortion caused by the photocyclization does not change the kinetic

(10) See Banman, A. T.; Chateauneuf, G. M.; Boyd, B. R.; Brown, R. E.; Murthy, P. P. N. *Tetrahedron Lett.* **1999**, *40*, 4489−4492, and references therein.
(11) Anet, F. A. L.; Schenck, G. E. *Tetrahedron Lett.* **1970**, *48*, 4237−4240.
(12) Hrovat, D. A.; Brown, E. C.; Williams, R. V.; Quast, H.; Borden, W. T. *J. Org. Chem.* **2005**, *70* (7), 2627−2632.
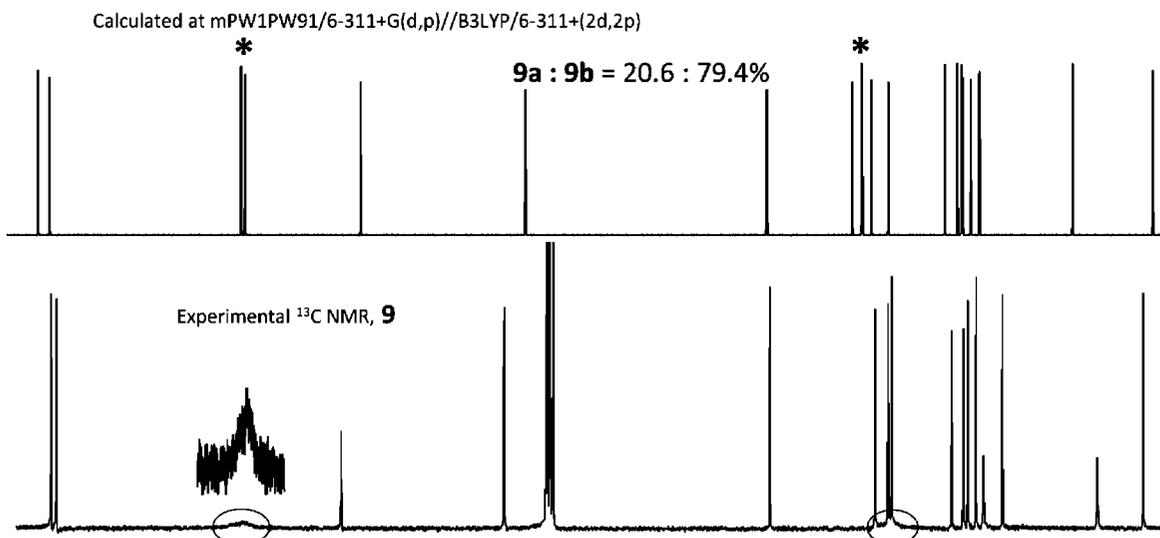
FIGURE 5. Calculated (top) and experimental (bottom) ^{13}C NMR spectra of **9**. Asterisks (*) show the predicted positions for signals of the averaged carbon atoms α, α' and γ, γ', which match the broad peaks in the experimental spectrum (circled).

barrier. The computed value of 7.5−7.6 kcal/mol is somewhat smaller than the one predicted by our experimental estimates and smaller than the 9.5 kcal/mol reported for dihydrobullvalene.[11] We note that Borden's DFT calculations on the parent dihydrobullvalene at B3LYP/6-31G(d) level also yielded an underestimated barrier of 8.5 kcal/mol.[12] In our calculation this lower level of theory gave a seemingly better estimate of the activation barrier (9.6−9.7 kcal/mol, first entry in Table 1).

The effect of the photodistortion on the relative stabilities of the two Cope states **9a** and **9b** can be rationalized in terms of unfavorable interaction between the alkenyl moiety and the nearest proton residing on the cyclobutane moiety (Figure 6).

As the first projection in Figure 6 shows, the vinyl-cyclopropane moiety is "slimmer" at the cyclopropyl terminus by approximately 1 Å compared with the open alkenyl terminus. This wedged shape is responsible for the steric discrimination upon twisting the dihedral angle a−b−c−d, as a result of the oxetane formation. Such twisting sets the proton H_a of the cyclobutyl moiety on a collision course with the cyclopropenyl terminus in B or with the alkenyl moiety as in A. Due to the wedged geometry the alkenyl moiety is much closer, and therefore such a distortion of the structure A leads to unfavorable steric interaction, which is less pronounced in B.

We quantitatively evaluated this effect in the truncated cyclobutanodihydrobullvalene moiety using a B3LYP/6-311+G(d,p) relaxed scan of the dihedral a−b−c−d. Figure 7 summarizes the effect of twisting the dihedral angle on (i) the relative energies of two "isomers" A and B (the truncated moieties A and B are enantiomers, but **9a** and **9b** are diastereomers) and (ii) the distances between protons H_a and H_d and the cyclopropyl or the vinyl carbons α and γ.

As the dihedral angle φ_{abcd} was scanned from 0° to 20°, the relative energy of the "isomer" A steadily increases, because the proton H_a is being forced into the alkenyl carbon: the initial distance is 2.72 Å, and after 10° twisting the distance is halted at 2.6 Å while the energy increases dramatically. In the isomer B, proton H_a initially (i.e., at $\varphi_{abcd} = 0°$) is at a comfortable 3.2 Å from the cyclopropyl moiety. Although proton H_d is initially at 2.72 Å in this conformation (filled circles in the right pane of Figure 7), it is being rotated away from the alkenyl terminus with the distance steadily increasing to 3.2 Å. The implication
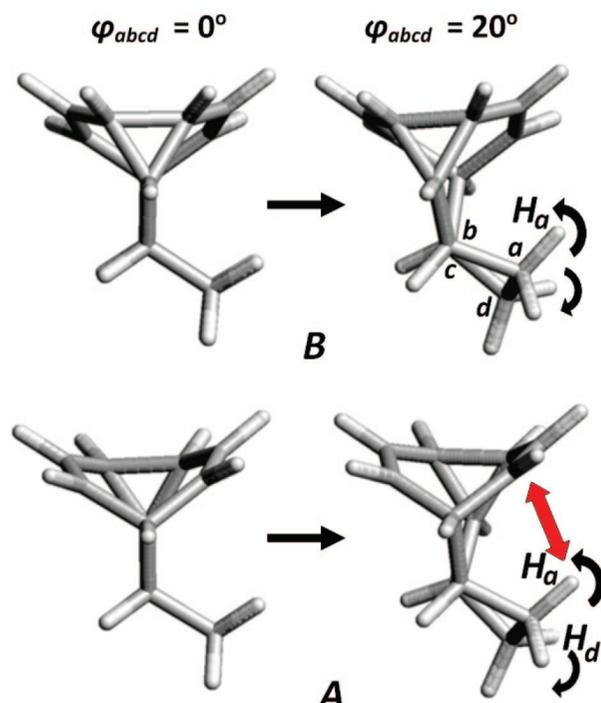
FIGURE 6. Cyclobutanodihydrobullvalene structure as the dihedral angle a−b−c−d is being scanned. In the less stable valence isomer (A) the proton H_a is rammed into the proximal alkene terminus.

of this motion in the case of B is that for the first 8° of twisting the energy actually relaxes somewhat before raising again at the larger values of φ_{abcd}. That is, the initial twisting stabilizes the isomer B and destabilizes the isomer A.

As it is mentioned above, both the X-ray structural data and the DFT calculations indicate that the distortion introduced by the Paternò−Büchi reaction translates into a φ_{abcd} value of 9.7−9.8°. According to the relaxed scan in Figure 7 this happens to be an optimal value for the *maximum* energy gap between the two valence isomers. It is curious that in this system the distortion, introduced by a photochemical reaction at the remote terminus of the molecule, propagates to the cyclobutane bridge and settles at the best possible twisting angle value to produce the most pronounced effect on the NMR spectrum (Figure

FIGURE 7. (Left) DFT energy change as a function of the dihedral angle φ_{abcd} in the cyclobutanodihydrobullvalene moiety. (Right) Distance between the respective *endo*-cyclobutano hydrogens and the α,γ carbons of the Cope system in isomers A (triangles) and B (circles): to the cyclopropyl carbon, open markers; to the alkenyl carbon, solid markers.

2) of this fluxional system. Potentially, as the oxetane formation can be made reversible either thermally[13] or photochemically,[14] this system may offer a way of controlling molecular properties with a photoinduced switch.

Experimental Section

Computational Details. DFT computations were carried out with Gaussian 03, rev. E.01 (for reference see Supporting Information). The geometries were optimized at the B3LYP/6-311+G(d,p) level; all stationary points were characterized by vibrational analysis to correct for ZPE and test for imaginary frequencies. The NMR chemical shifts and spin–spin coupling constants were computed at the mPW1PW91 level of theory using a variety of basis sets, of which 6-311+G(d,p) was optimal.

General Procedure for Synthesis of Diels–Alder Adducts. A dienophile and cyclooctatetrane in 1,2-dichlorobenzene (DCB) was heated in a pressure vessel at 180–200 °C for 1–2 days and cooled to room temperature, and the solvent was removed on a high vacuum pump. The adducts were purified by chromatography on slurry packed silica gel columns using gradient elution with ethyl acetate–hexane.

Methyl Vinyl Ketone Adduct 6. COT (2.0 g, 19.2 mmol) and 3.2 mL of methyl vinyl ketone (38.4 mmol) in 7 mL of DCB was heated at 180 °C for 48 h. Gradient elution in ethyl acetate–hexane (1:30 → 1:20). *endo*-adduct **6**: 1.1 g, 41% yield. ^{1}H NMR (400 M Hz, CDCl$_3$) δ 6.35 (1H, t, J = 7.5 Hz), 6.14 (1H, t, J = 7.5 Hz), 5.93 (1H, t, J = 9.5 Hz), 5.68 (1H, t, J = 9.5 Hz), 3.6–3.9 (4H, m), 2.89 (1H, m), 2.59 (1H, m), 2.47 (1H, ddd, J = 9.7, 5.2, 2.0 Hz), 2.3 (1H, m), 2.22 (1H, m), 2.15 (1H, m), 2.10 (1H, m), 2.09 (3H, s), 1.872 (1H, t, J = 8.7 Hz), 1.87 (1H, t, J = 8.7 Hz), 1.67 (1H, ddd, J = 12.6, 5.2, 3.2 Hz), 1.42 (1H, ddd, J = 12.4, 9.7, 2.5 Hz). ^{13}C NMR (400 M Hz, CDCl$_3$) δ 209.8, 135.0, 130.5, 126.70, 126.3, 50.3, 44.5, 43.6, 37.0, 36.5, 36.0, 33.5, 28.7, 28.3, 28.0, 26.8. GCMS m/z 43 (26), 91 (100), 115 (20), 129 (23), 235 (16), 278 (M+, 1). HRMS (ESI) calcd for C$_{20}$H$_{22}$ONa$^+$ (MNa$^+$) 301.1562, found 301.1550. *exo*-adduct **6**′: ^{1}H NMR (400 M Hz, CDCl$_3$) δ 6.42 (1H, t, J = 7.3 Hz), 6.36 (1H, t, J = 7.3 Hz), 5.88 (1H, t, J = 9.5 Hz), 5.66 (1H, t, J = 9.5 Hz), 3.79–3.55 (4H, m), 2.85 (1H, m), 2.55 (1H, m), 2.44 (1H, ddd, J = 11.0, 5.2, 2.3 Hz), 2.25–2.1 (5H, m), 2.14 (3H, s), 1.8 (2H, m), 1.3 (1H, m). ^{13}C NMR (400 M Hz, CDCl$_3$) δ 209.8, 135.1, 133.5, 126.7, 126.3, 50.6, 43.5, 39.6, 37.4, 37.3, 35.7, 33.3, 29.2, 28.6, 27.6, 25.7. GCMS m/z 43 (21), 71 (18), 91 (100), 115 (18), 129 (24), 207 (11), 235 (11), 278 (M+, 1).

Cyclohexenone Adduct 7. COT (2.0 g, 19.2 mmol) and 0.93 mL of 2-cyclohexene-1-one (9.60 mmol) in 7 mL of DCB was heated at 190 °C for 24 h. Gradient elution in ethyl acetate–hexane (1:25 → 1:15): 11% (0.3 g) yield. ^{1}H NMR (400 M Hz, CDCl$_3$) δ 6.34 (1H, t, J = 7.3 Hz), 6.19 (1H, t, J = 7.3 Hz), 5.92 (1H, t, J = 9.6 Hz), 5.67 (1H, t, J = 9.6 Hz), 3.82 (2H, br. s), 3.70 (2H, br. s), 3.08 (1H, m), 2.46 (1H, m), 2.3–2.1 (9H, m), 1.9–1.7 (4H, m), 0.96 (1H, m). ^{13}C NMR (400 M Hz, CDCl$_3$) δ 214.64, 134.29, 132.87, 126.68, 126.24, 53.66, 51.64, 44.45, 42.93, 41.06, 39.73, 39.10, 36.72, 36.56, 35.06, 29.77, 28.21 (broadened), 28.10 (broadened), 21.06 (in all compounds four carbons averaged by the [3,3]-sigmatropic shift are not discernible). HRMS (ESI) calcd for C$_{22}$H$_{24}$ONa$^+$ (MNa$^+$) 327.1719, found 327.1712.

Dibenzoyl Adducts 4 and 5. A mixture of 3.00 g of COT (28.80 mmol) and 6.80 g of *trans*-1,2-dibenzoylethylene (28.80 mmol) in 30 mL of DCB was heated at 190 °C for 48 h. Gradient elution in ethyl acetate–hexane (1:50 → 1:30): (a) Mono-adduct **4**: 14% (1.41 g) yield. ^{1}H NMR (400 M Hz, CDCl$_3$) δ 7.99 (4H, m), 7.55 (2H, m), 7.46 (4H, m), 6.20 (1H, t, J = 7.3 Hz), 5.84 (1H, t, J = 7.3 Hz), 5.76 (2H, br. s), 4.43 (1H, dd, J = 5.5, 2.0 Hz), 4.32 (1H, dd, J = 5.3, 2.6 Hz), 3.14 (1H, t, J = 3.7 Hz), 3.06 (1H, m), 3.01 (1H, m), 2.70 (1H, t, J = 3.6 Hz). ^{13}C NMR (400 M Hz, CDCl$_3$) δ 201.1, 200.8, 138.3, 137.5, 136.9, 136.6, 133.3, 133.1, 130.0, 128.9, 128.9, 128.7, 128.7, 128.1, 47.4, 45.5, 45.1, 41.2, 39.2, 38.7. GCMS m/z 77 (60), 105 (100), 262 (33), 235 (18), 340 (M+, 3.5). HRMS (ESI) calcd for C$_{24}$H$_{21}$O$_2^+$ (MH$^+$) 341.1536, found 341.1522. (b) Bis-adduct **5** (for the X-ray structure see Supporting Information): ^{1}H NMR (400 M Hz, CDCl$_3$) δ 8.01 (2H, d, J = 7.9 Hz), 7.95 (2H, d, J = 7.9 Hz), 7.58–7.42 (6H, m), 6.58 (1H, t, J = 7.4 Hz), 6.18 (1H, t, J = 9.5 Hz), 4.26 (1H, dd, J = 5.7, 1.8 Hz), 4.18 (1H, dd, J = 5.6, 2.5 Hz), 3.92 (1H, br. s), 3.72 (2H, br. s), 3.6 (1H, br. s), 2.98 (2H, m), 2.65 (1H, m), 2.22 (1H, m), 2.13 (2H, m), 1.89 (1H, m, J = 8.7, 8.7, 4.5 Hz), 1.70 (1H, m, J = 8.7, 8.7, 4.5 Hz). ^{13}C NMR (400 M Hz, CDCl$_3$) δ 201.0, 200.2, 136.7, 136.6, 134.0, 133.2, 133.1, 131.8, 128.9, 128.8, 128.8, 128.7, 126.7, 126.5, 47.0, 45.1, 43.5, 38.8, 38.1, 37.6, 36.8, 36.7, 28.1, 27.8. GCMS m/z 51 (21), 77 (64), 105 (100), 157 (10), 235 (16) 262 (26). HRMS (ESI) calcd for C$_{32}$H$_{29}$O$_2^+$ (MH$^+$) 445.2162, found 445.2175.

Paternò–Büchi Reaction. A dilute DCM solution of the Diels–Alder adducts was irradiated in quartz (**6**) or Pyrex (**5**) vials for 24–48 h. Irradiations were carried out in a Rayonet photoreactor using RPR-3000 UV lamps (broadband 250–350 nm sources with peak emission at 300 nm). The RPR-3500 UV lamps (broadband 300–400 nm sources with peak emission at 350 nm) can also be used for the aromatic ketones. After photolysis the solvent was removed and the reaction mixtures were purified by chromatography (silica gel, ethyl acetate and hexane).

Oxetane 9. From 1.10 g of **6** (3.95 mmol); gradient elution with ethyl acetate–hexane (1:30 → 1:10); 0.34 g (31%); ^{1}H NMR (400 M Hz, CDCl$_3$) δ 5.93 (1H, dd, J = 10.6, 8.1 Hz), 5.72 (1H, dd, J

(13) (a) Jones, G.; Acquadro, M. A.; Carmody, M. A. *J. Chem. Soc., Chem. Commun.* **1975**, (6), 206–207. (b) Jones, G.; Schwartz, S. B.; Marton, M. T. *J. Chem. Soc., Chem. Comm.* **1973**, (11), 374–375.

(14) Perez-Ruiz, R.; Miranda, M. A.; Alle, R.; Meerholz, K.; Griesbeck, A. G. *Photochem. Photobiol. Sci.* **2006**, *5* (1), 51–55.

= 10.7, 8.1 Hz), 5.19 (1H, br. t) 5.00 (1H, br. t), 4.72 (1H, m), 2.81 (1H, m), 2.66 (1H, m, J = 8.8, 8.8, 5.0 Hz), 2.48 (3H, m), 2.40 (1H, m), 2.34 (1H, m, J = 10.0, 3.5, 3.5 Hz), 2.28 (1H, m, J = 9.5, 3.6, 3.6 Hz), 2.17 (1H, m, J = 8.6, 8.6, 4.0 Hz), 2.05 (1H, d, J = 6.3 Hz), 1.82 (1H, m), 1.69 (2H, m), 1.48 (3H, s), 1.33 (1H, d, J = 11.9 Hz). ^{13}C NMR (400 M Hz, CDCl$_3$) δ 127.1, 126.6, 108.0 (broadened), 98.1, 81.8, 55.3, 44.7, 43.4, 43.0, 43.0 (broadened), 37.1, 35.9, 35.5, 34.6, 33.8, 32.0, 22.5, 17.9. GCMS *m/z* 43 (21), 91 (100), 129 (29), 235 (9), 278 (M+, 1). HRMS (ESI) calcd for C$_{20}$H$_{22}$ONa$^+$ (MNa$^+$) 301.1562, found 301.1567.

Oxetane 8. (For X-ray structure, see Supporting Information) ^{1}H NMR (400 M Hz, CDCl$_3$) δ 7.76 (2H, d, J = 7.6 Hz), 7.56−7.35 (8H, m), 5.69 (2H, dd, J = 10.4, 8.4 Hz), 5.16 (1H, br. t), 4.99 (1H, br. t), 3.59 (1H, m), 3.54 (1H, dd, J = 6.7, 1.2 Hz), 3.20 (1H, d, J = 6.3 Hz), 2.85 (1H, m), 2.57 (2H, m), 2.41 (2H, m), 2.15 (2H, m), 1.51 (1H, m, J = 8.8, 8.8, 6.2 Hz). ^{13}C NMR (400 M Hz, CDCl$_3$) δ 201.3, 137.6, 137.0, 132.9, 129.1, 128.9, 128.8, 127.8, 127.5, 126.8, 126.5, 97.3, 81.9, 55.7, 55.1, 45.4, 43.2, 39.5, 37.6, 37.3, 36.7, 35.4, 33.7, 22.1. GCMS *m/z* 106 (9), 203 (100), 352 (11). HRMS (ESI) calcd for C$_{32}$H$_{29}$O$_2^+$ (MH$^+$) 445.2162, found 445.2176.

Oxetane 10. ^{1}H NMR (400 M Hz, CDCl$_3$) δ 5.91 (1H, dd, J = 10.6, 8.0 Hz), 5.70 (1H, dd, J = 10.5, 8.1 Hz), 5.13 (1H, t, J = 9.3 Hz), 4.94 (1H, t, J = 9.2 Hz), 4.74 (1H, m), 2.69 (1H, m), 2.65 (1H, m), 2.51 (2H, m), 2.42 (1H, m), 2.34 (1H, m), 2.27 (1H, m), 2.14 (1H, ddd, J = 8.6, 8.6, 3.9 Hz), 1.95−1.8 (7H, m), 1.75−1.65 (2H, m), 1.5−1.25 (2H, m). ^{13}C NMR (400 M Hz, CDCl$_3$) δ 127.3, 126.8, 98.90, 82.9, 48.5, 46.7, 44.0, 43.4, 38.4, 37.2, 36.2, 36.1, 34.1, 30.3, 29.9, 29.6, 22.9, 21.1.

Supporting Information Available: NMR spectra (^{1}H ^{13}C, COSY, NOE), VT NMR experiments, X-ray data, and computational details. This material is available free of charge via the Internet at http://pubs.acs.org.

JO9003822